Chemically Resolved Transient Collision Events of Single Electrocatalytic Nanoparticles

Zhihui Guo,[†] Stephen J. Percival, and Bo Zhang*

Department of Chemistry, University of Washington, Seattle, Washington 98195-1700, United States

S *Supporting Information*

ABSTRACT: Here we report the use of fast-scan cyclic voltammetry (FSCV) to study transient collision and immobilization events of single electrocatalytic metal nanoparticles (NPs) on an inert electrode. In this study, a fast, repetitive voltage signal is continuously scanned on an ultramicroelectrode and its faradaic signal is recorded. Electrocatalytically active metal NPs are allowed to collide and immobilize on the electrode resulting in the direct recording of the transient voltammetric response of single NPs. This approach enables one to obtain the transient voltammetric response and electrocatalytic effects of single catalytic NPs as they interact with an inert electrode. The use of FSCV has enabled us to obtain chemical information, which is otherwise difficult to study with previous amperometric methods.

Scheme 1. FSCV Detection of Single-Particle Collision

Metal nanoparticles (NPs) find wide application in studies including biotechnology[1,2] and sensing[3,4] and are the materials of choice in numerous electrocatalytic processes.[5−7] This is at least partially due to their unique size and shape tunable electronic, optical, and catalytic properties.[8−11] Previous research in the area of NP electrochemistry and electrocatalysis has mainly studied the structure−function relationships of NP ensembles.[10,12] This, however, is challenging due to ensemble averaging and possible overlap in the diffusion field in closely spaced NPs.[13] The ability to directly analyze structurally well-characterized single particles opens up new avenues in this area.

A number of excellent single-particle experiments have recently been published. These include experiments utilizing transient particle-electrode collision[14] and catalytic amplification,[15−18] single-molecule fluorescence,[19] and surface plasmon spectroscopy.[20] Fluorescence and surface plasmon based methods allow a single-NP response to be optically addressed from an ensemble allowing many particles to be studied simultaneously.[21] Direct electrical measurements generally require isolation of individual particles from the bulk. There are three major ways to isolate single NPs: particle−electrode collision,[15−18] single-particle immobilization on a nanoelectrode,[22,23] and methods based on the use of a scanning probe.[24] We, along with others,[25] have used nanoelectrodes to isolate, immobilize, and characterize single metal NPs.

Single-particle collision has become a particularly useful approach because of its simplicity, speed, and power allowing for quick analysis of hundreds of NPs in minutes. Previous particle collision experiments involve holding a constant potential on a probe ultramicroelectrode (UME) and recording
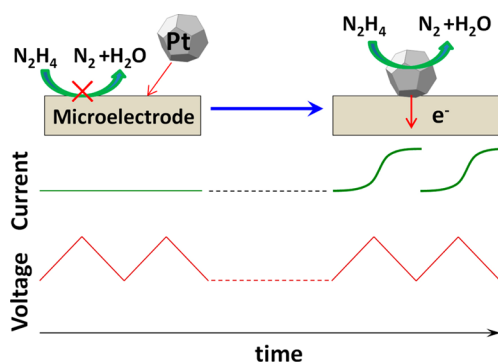
its time-dependent faradaic response as single particles interact with the electrode. Each NP collision event results in a transient current fluctuation due to catalytic current amplification[16] or current blockage.[26] A limitation of this approach, however, is the lack of chemical resolution. As such, its application has been primarily limited to the study of highly pure NPs at a fixed potential where no additional information is gained beyond the transient current response.

We have been working on a new approach to extend the single-particle collision concept to better understand the transient interfacial kinetics of NPs. Our approach is based on the use of a fast and repetitive voltage perturbation on an inert electrode to obtain a transient electrocatalytic response during collision events of single NPs. Our goal is to gain necessary chemical information on single NPs undergoing quick collisions. This study will likely extend the use of the powerful particle−electrode collision approach to uncovering some of the hidden details of the electrocatalytic process.

Our approach involves the use of fast-scan cyclic voltammetry (FSCV) and is illustrated in Scheme 1. In this work, a popular electrocatalytic amplification scheme has been adopted, which consists of a 5 μm diameter carbon-fiber UME as the probe electrode, 15 mM hydrazine (H_4N_2) as the redox indicator, and platinum and gold NPs. Here, a triangular voltage waveform is continuously scanned on the probe UME and the background-subtracted faradaic response is monitored. The voltage on the UME is scanned in a range typically between −0.4 and +0.4 V vs a Ag/AgCl electrode where oxidation of hydrazine is kinetically slow on carbon but can be catalytically enhanced on platinum or gold. When a platinum (or gold) NP approaches and attaches on
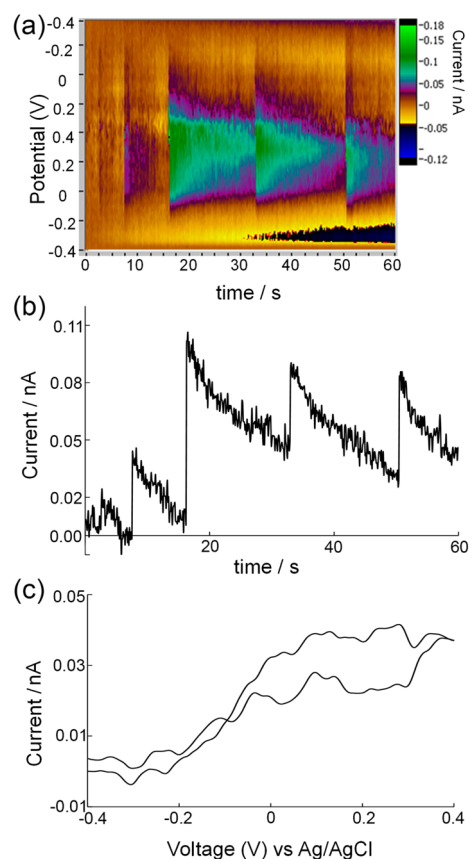
Figure 1. Single collisional events of platinum NPs on carbon. (a) A 60 s FSCV recording at $\nu = 400$ V/s showing detection of 5 Pt NPs on a 5 μm carbon UME in a 15 mM hydrazine solution. (b) The current−time trace taken from (a) at +0.1 V vs Ag/AgCl showing single-particle current peaks similar to that recorded with conventional amperometry. (c) Background-subtracted CV recorded at 7.7 s in (a) showing faradaic response of an ∼4 nm Pt particle.

the carbon UME, hydrazine oxidation can quickly proceed on the NP resulting in a sudden, drastic increase in the faradaic signal.[16,17] It is important to note that FSCV is a popular electroanalytical technique pioneered by Wightman and co-workers[27,28] and is particularly useful in the study of fast neurochemical events in the brain.

Figure 1a displays a characteristic 60 s FSCV trace recorded on a 5 μm diameter carbon UME in a solution containing 15 mM H_4N_2, 5 mM phosphate at pH 7.4, and 0.5 nM 4 nm platinum NPs (Figure S1). Here, a color plot is employed to present 6000 continuously recorded, background-subtracted CVs together in one figure. The current is color-coded, and the electrode potential is plotted on the y-axis. Additional details about FSCV and the use of color plots can be found in a recent article by Wightman and co-workers.[29] A NP collision event in Figure 1a is represented by a quick color (current) change. Here, five discrete collision events, at approximately 2.5, 7.5, 17, 33, and 51 s, respectively, are clearly resolved. Each event shows distinct voltammetric characteristics indicating that they are from different particles and not the same particle bouncing back and forth on the electrode. Here, the rate at which Pt particles are detected is smaller than that predicted from diffusion flux (Supporting Information (SI)) indicating that only a small number of particles reaching the electrode result in effective detection.

The faradaic current at a certain applied potential from each individual CV can be easily extracted out of the color plot to generate a current−time response similar to that recorded in conventional amperometry. Figure 1b is the current−time trace at 0.1 V obtained from Figure 1a where Figure 1b has kept some of the essential characteristics of single NP collision events of Pt in hydrazine. Each particle collision event can be seen as a quick increase in the faradaic current originating from the electro-catalytic amplification of platinum on carbon. The drop in current is believed to be largely due to particle deactivation although the exact mechanism is unclear. A similar response has been observed in constant-potential amperometry, as shown in Figure S2.

Figure 1c shows a background-subtracted CV response recorded at 7.7 s, which corresponds to immediately after collision and immobilization of a second Pt NP in this 60 s trace. The current−voltage response at 7.5, right before the sharp current increase, was used as the background. The collision event results in a sigmoidal shape CV response which is due to the electrocatalytic oxidation of hydrazine on the Pt. Interestingly, even at a scan rate of $\nu = 400$ V/s, the voltammetric response still displays steady-state behavior. This is due to fast and radial-type diffusion of hydrazine and kinetic limitation. First, a quick estimate (see SI) using the Einstein relation,[30] $d = (2Dt)^{1/2}$, gives a diffusion layer thickness d of 422 nm.[31] Here, $D = 1.39 \times 10^{-5}$ cm^2/s is the diffusion coefficient of hydrazine,[32] $t = RT/F\nu$ is the experimental time duration, R is the gas constant, T is the temperature, and F is the Faraday constant. This is more than 2 orders of magnitude greater than the radius of the NP. This gives rise to a radial type diffusion and sigmoidal shape voltammo-gram.[31] Second, the peak current in Figure 1b or the plateau current in Figure 1c is smaller than the theoretical prediction based on the diffusion limitation (see below), indicating that the hydrazine oxidation on Pt is kinetically limited due to the presence of citrate ligand molecules.

We have compared the faradaic responses recorded using both FSCV and amperometry in order to further validate the use of FSCV to study single particle collisions, and the results are shown in Figure 2. Here, a 5 μm carbon UME, 15 mM H_4N_2, and 0.5 nM 4 nm Pt particles were used. The hydrazine oxidation peak currents were recorded at the same voltage, +0.1 V vs Ag/AgCl. The FSCV histogram closely matches that of amperometry and the Gaussian fitting gives an average peak current of ∼36 pA in both cases, indicating that FSCV gives comparable electro-catalytic results in particle collisions. More importantly, FSCV
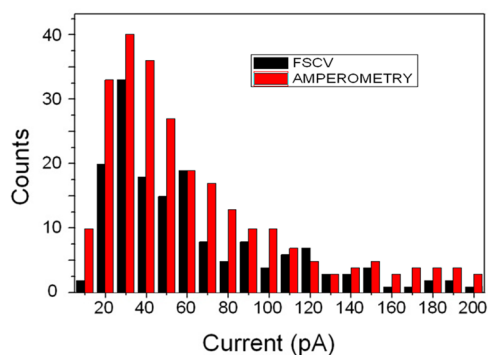
Figure 2. A comparison of peak current recorded in amperometry and FSCV for single-particle collision experiments. Here, all currents were recorded at +0.1 V vs Ag/AgCl on a 5 μm carbon UME. Both experiments used a 15 mM hydrazine solution and 0.5 nM 4 nm Pt NPs.

also offers additional chemical resolution, which is otherwise difficult to obtain with amperometry. This is further demonstrated in the following section.

We note that the average peak current is a bit smaller than the theoretical prediction (∼140 pA) based on the diffusion limitation,

$$i_{ss} = 4\pi \ln(2) nFDCr \qquad (1)$$

where i_{ss} is the diffusion limited hydrazine current, $n = 4$ is the number of electrons transferred per molecule, C is the bulk concentration, and r is the NP radius. There are three possible reasons leading to this smaller peak current. First, hydrazine is an inner-sphere redox molecule, and its oxidation on Pt surface may be strongly hindered by the presence of the ligand molecules on the NP.[33] Therefore, not all the surface area is available for hydrazine oxidation. Second, the measurement of the peak current may be affected by a quick deactivation of the Pt surface, as the NP is in close contact with the UME surface. Third, the high mass transfer on the NP could lead to partial decomposition of hydrazine and some of the reaction intermediates can be carried away by quick diffusion leading to a smaller apparent number of transferred electrons, n. Similar effects have been discussed in the literature for the reduction of oxygen on nanometer-scale electrodes.[25]

As expected, the use of FSCV is not restricted to the study of platinum NPs. Single-particle collisions can also be probed for gold particles on carbon UMEs with FSCV. The gold particles used in this work are citrate-stabilized, 12 nm spherical particles (Figure S1).

Figure 3a shows an FSCV color plot collected on a 5 μm carbon UME in a 15 mM H_4N_2 solution containing 0.1 nM 12 nm gold particles. Five collision events have been detected and
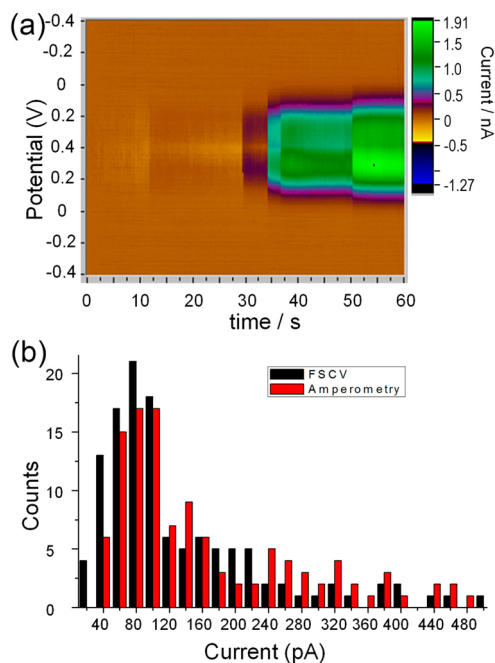
Figure 3. Single collisional events of 12 nm gold particles on carbon in a 15 mM hydrazine solution. (a) A 60 s FSCV color plot showing detection of gold particles on a 5 μm carbon UME. (b) A histogram of peak current detected with FSCV (black) and amperometry (red) for the same 12 nm gold particles in 15 mM hydrazine. The current was recorded at 0.2 V in both experiments.

are resolved on the color plot. Figure S3 shows a characteristic CV recorded from a 12 nm gold particle. Figure S4a is the current−time trace taken from the FSCV color plot at 0.2 V vs Ag/AgCl further illustrating the five collision events. As a comparison, Figure S4b is a current−time trace collected at the same voltage using amperometry. Discrete particle collisions have been clearly seen in both methods. Figure 3b is a comparison of peak current collected using both methods, and the results again show a good agreement between two detection methods in the distribution of event characteristics. Both methods have similar peak current distributions with the Gaussians centered at ∼80 pA. This peak current is also smaller than the theoretical prediction (∼420 pA) based on eq 1 and the particle size measured in TEM, and we hypothesize that this is due to the same possible factors: hindrance from ligands, particle deactivation, and high mass-transport rate.

The voltage scan rate, ν, is an important parameter in FSCV and should be carefully selected in a particular collision experiment. The scan rate can have several key effects. First, it is directly related to the temporal resolution, and therefore, a high ν is preferred because it allows for a higher repetition rate, i.e. number of CVs per unit time, and thus increased temporal resolution. Second, one would think that it may affect the faradaic current collected on the NP. Our results have shown (Figure S5) that the faradaic response recorded with FSCV is essentially independent of scan rate due to the extremely small size of NPs and high mass transfer rate. We normally use scan rates in the range of 50−500 V/s, and the characteristic radial-type diffusion is expected to be maintained. Third, the voltage scan rate cannot be too high because the double layer charging current increases linearly with scan rate. Therefore, depending on the size of the probe UME, it may cause extra noise or even current overload.

One of the most significant features of FSCV is its excellent chemical resolution in addition to high temporal resolution. Wightman and co-workers have reported that it is possible to identify up to 9 different redox species in a 2-V CV scan.[34] Here, chemical resolution is also demonstrated in this study using a mixed solution containing platinum and gold NPs. We note that a mixed solution of Pt and Au particles is not chemically stable and one can often see quick color changes indicating particle aggregation upon mixing. Figure 4a is an FSCV color plot recorded on a 5 μm carbon electrode in a 5 mM phosphate buffer containing 15 mM N_2H_4, 0.1 nM 12 nm gold NPs, and 0.1 nM 30 nm platinum NPs. There are 11 collision events detected in this 60 s detection period. Each NP collision event can be individually examined to extract its CVs prior to and after particle immobilization. A careful analysis of their voltammetric responses reveals that both platinum and gold NPs were detected: events 2, 3, 8, 9, and 10 are likely due to platinum NPs with a representative CV shown in Figure 4b (blue); events 4 and 5 are likely due to gold NPs, Figure 4b (black). Interestingly, a few events exhibited characteristics of both metals, likely due to the collision of gold−platinum dual particles, where Pt NPs may have adsorbed onto the Au NPs before collision. These include events 1, 6, 7, and 11. There are two consecutive oxidation waves seen in the CV as shown in the red curve in Figure 4b. The first wave at ∼ −0.2 V is likely due to platinum, and the second wave at +0.2 V is likely due to the presence of gold.

In conclusion, we have presented the use of fast-scan cyclic voltammetry to study single-nanoparticle collisions and immobilization on an inert ultramicroelectrode. This method uses a scanning potential on an inert UME at high scan and repetition rates and records its faradaic response as single electrocatalytic
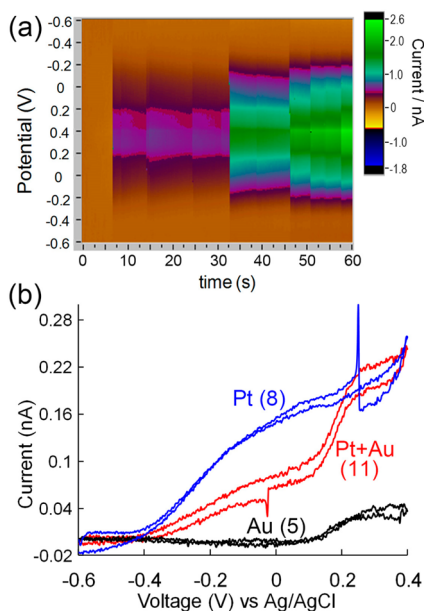
Figure 4. Chemically resolving single NPs. (a) A 60 s FSCV color plot showing detection of 11 single collision events on a 5 μm carbon UME in a 15 mM hydrazine solution. (b) Typical single-particle CVs recorded with FSCV. The blue, red, and black CVs are extracted from particles 8, 11, and 5 respectively.

metal NPs undergo stochastic collision processes with the electrode surface. The use of FSCV has enabled us to obtain chemically resolved information about transient particle–electrode interactions which is otherwise difficult to obtain with previous constant-potential techniques. Voltammetric responses can be obtained at single colliding NPs with millisecond time resolution prior to and after particle collision and immobilization. Such information can be particularly valuable for future mechanistic studies for electrocatalytic NPs such as particle–electrode interaction, particle activation and deactivation, and heterogeneous electron-transfer kinetics. These are among the subjects of our ongoing studies.

■ ASSOCIATED CONTENT

Ⓢ Supporting Information

Chemicals and materials, instruments, experimental details, TEM images of gold and platinum NPs, more FSCV and amperometry data as mentioned in the main text. This material is available free of charge via the Internet at http://pubs.acs.org.

■ AUTHOR INFORMATION

Corresponding Author

zhang@chem.washington.edu

Present Address

†Z.G.: School of Chemistry & Chemical Engineering, Shaanxi Normal University, Xi'an 710062, P.R. China

Notes

The authors declare no competing financial interest.

■ ACKNOWLEDGMENTS

■ REFERENCES

(1) Rosi, N. L.; Giljohann, D. A.; Thaxton, C. S.; Lytton-Jean, A. K. R.; Han, M. S.; Mirkin, C. A. *Science* **2006**, *312*, 1027.

(2) Rand, D.; Ortiz, V.; Liu, Y.; Derdak, Z.; Wands, J. R.; Tatíček, M.; Rose-Petruck, C. *Nano Lett.* **2011**, *11*, 2678.

(3) Polsky, R.; Gill, R.; Kaganovsky, L.; Willner, I. *Anal. Chem.* **2006**, *78*, 2268.

(4) Tseng, S.-C.; Yu, C.-C.; Wan, D.; Chen, H.-L.; Wang, L. A.; Wu, M.-C.; Su, W.-F.; Han, H.-C.; Chen, L.-C. *Anal. Chem.* **2012**, *84*, 5140.

(5) Crooks, R. M.; Zhao, M.; Sun, L.; Chechik, V.; Yeung, L. K. *Acc. Chem. Res.* **2001**, *34*, 181.

(6) Tian, N.; Zhou, Z.-Y.; Sun, S.-G.; Ding, Y.; Wang, Z. L. *Science* **2007**, *316*, 732.

(7) Shao, M.; Odell, J.; Humbert, M.; Yu, T.; Xia, Y. *J. Phys. Chem. C* **2013**, *117*, 4172.

(8) Daniel, M.-C.; Astruc, D. *Chem. Rev.* **2004**, *104*, 293.

(9) Somorjai, G. A.; Li, Y. *Introduction to Surface Chemistry and Catalysis*, 2nd ed.; John Wiley & Sons: Hoboken, NJ, 2010.

(10) Burda, C.; Chen, X.; Narayanan, R.; El-Sayed, M. A. *Chem. Rev.* **2005**, *105*, 1025.

(11) Ye, H.; Crooks, J. A.; Crooks, R. M. *Langmuir* **2007**, *23*, 11901.

(12) Chen, M.; Goodman, D. W. *Acc. Chem. Res.* **2006**, *39*, 739.

(13) Watanabe, M.; Sei, H.; Stonehart, P. *J. Electroanal. Chem.* **1989**, *261*, 375.

(14) Fosdick, S. E.; Anderson, M. J.; Nettleton, E. G.; Crooks, R. M. *J. Am. Chem. Soc.* **2013**, *135*, 5994.

(15) Xiao, X.; Bard, A. J. *J. Am. Chem. Soc.* **2007**, *129*, 9610.

(16) Xiao, X.; Fan, F.-R. F.; Zhou, J.; Bard, A. J. *J. Am. Chem. Soc.* **2008**, *130*, 16669.

(17) Dasari, R.; Robinson, D. A.; Stevenson, K. J. *J. Am. Chem. Soc.* **2013**, *135*, 570.

(18) Zhou, Y.-G.; Rees, N. V.; Compton, R. G. *Angew. Chem., Int. Ed.* **2011**, *50*, 4219.

(19) Zhou, X.; Andoy, N. M.; Liu, G.; Choudhary, E.; Han, K.-S.; Shen, H.; Chen, P. *Nat. Nanotechnol.* **2012**, *7*, 237.

(20) Shan, X.; Díez-Pérez, I.; Wang, L.; Wiktor, P.; Gu, Y.; Zhang, L.; Wang, W.; Lu, J.; Wang, S.; Gong, Q.; Li, J.; Tao, N. *Nat. Nanotechnol.* **2012**, *7*, 668.

(21) Zhou, X.; Choudhary, E.; Andoy, N. M.; Zou, N.; Chen, P. *ACS Catal.* **2013**, *3*, 1448.

(22) Li, Y.; Cox, J. T.; Zhang, B. *J. Am. Chem. Soc.* **2010**, *132*, 3047.

(23) Sun, P.; Li, F.; Yang, C.; Sun, T.; Kady, I.; Hunt, B.; Zhuang, J. *J. Phys. Chem. C* **2013**, *117*, 6120.

(24) Tel-Vered, R.; Bard, A. J. *J. Phys. Chem. B* **2006**, *110*, 25279.

(25) Chen, S.; Kucernak, A. *J. Phys. Chem. B* **2004**, *108*, 3262.

(26) Quinn, B. M.; van 't Ho, P. G.; Lemay, S. G. *J. Am. Chem. Soc.* **2004**, *126*, 8360.

(27) Robinson, D. L.; Wightman, R. M. In *Electrochemical Methods for Neuroscience*; Michael, A. C., Borland, L. M., Eds.; CRC Press: Boca Raton, FL, 2007; pp 17

(28) Baur, J. E.; Kristensen, E. W.; May, L. J.; Wiedemann, D. J.; Wightman, R. M. *Anal. Chem.* **1988**, *60*, 1268.

(29) Bucher, E. S.; Brooks, K.; Verber, M. D.; Keithley, R. B.; Owesson-White, C.; Carroll, S.; Takmakov, P.; McKinney, C. J.; Wightman, R. M. *Anal. Chem.* **2013**, *85*, 10344.

(30) Berg, H. C. *Random Walk in Biology*; Princeton University Press: Princeton, NJ, 1993.

(31) Bard, A. J.; Faulkner, L. R. *Elecrochemical Methods*, 2nd ed.; John Wiley & Sons: New York, 2001.

(32) Karp, S.; Meites, L. *J. Am. Chem. Soc.* **1962**, *18*, 906.

(33) Bratlie, K. M.; Lee, H.; Komvopoulos, K.; Yang, P.; Somorjai, G. A. *Nano Lett.* **2007**, *7*, 3097.

(34) Heien, M. L. A. V.; Johnson, M. A.; Wightman, R. M. *Anal. Chem.* **2004**, *76*, 5697.